

Beam Collimation at Hadron Colliders*

N.V. Mokhov
FNAL, Batavia, IL 60510, USA

July 29, 2003

Abstract

Operational and accidental beam losses in hadron colliders can have a serious impact on machine and detector performance, resulting in effects ranging from minor to catastrophic. Principles and realization are described for a reliable beam collimation system required to sustain favorable background conditions in the collider detectors, provide quench stability of superconducting magnets, minimize irradiation of accelerator equipment, maintain operational reliability over the life of the machine, and reduce the impact of radiation on personnel and the environment. Based on detailed Monte-Carlo simulations, such a system has been designed and incorporated in the Tevatron collider. Its performance, comparison to measurements and possible ways to further improve the collimation efficiency are described in detail. Specifics of the collimation systems designed for the SSC, LHC, VLHC, and HERA colliders are discussed.

*Presented paper at the *ICFA Workshop on Beam Halo Dynamics, Diagnostics, and Collimation (HALO'03)*, Montauk, Long Island, NY, May 19-23, 2003

Beam Collimation at Hadron Colliders¹

N. V. Mokhov²

Fermilab, P.O. Box 500, Batavia, IL 60510, USA

Abstract. Operational and accidental beam losses in hadron colliders can have a serious impact on machine and detector performance, resulting in effects ranging from minor to catastrophic. Principles and realization are described for a reliable beam collimation system required to sustain favorable background conditions in the collider detectors, provide quench stability of superconducting magnets, minimize irradiation of accelerator equipment, maintain operational reliability over the life of the machine, and reduce the impact of radiation on personnel and the environment. Based on detailed Monte-Carlo simulations, such a system has been designed and incorporated in the Tevatron collider. Its performance, comparison to measurements and possible ways to further improve the collimation efficiency are described in detail. Specifics of the collimation systems designed for the SSC, LHC, VLHC, and HERA colliders are discussed.

INTRODUCTION

At hadron colliders, as at any other accelerator, the creation of beam halo is unavoidable. This happens because of beam-gas interactions, intra-beam scattering, proton-proton (antiproton) collisions in the interaction points (IP), and particle diffusion due to RF noise, ground motion and resonances excited by the accelerator magnet nonlinearities and power supplies ripple. As a result of halo interactions with limiting apertures, hadronic and electromagnetic showers are induced in accelerator and detector components causing numerous deleterious effects ranging from minor to severe. An accidental beam loss caused by an unsynchronized abort launched at abort system malfunction can cause catastrophic damage to the collider equipment. Only with a very efficient beam collimation system can one reduce uncontrolled beam losses in the machine to an allowable level [1, 2].

Beam collimation is mandatory at any superconducting hadron collider to protect components against excessive irradiation, minimize backgrounds in the experiments, maintain operational reliability over the life of the machine (quench stability among other things), and reduce the impact of radiation on the environment. It provides:

1. Reduction of beam loss in the vicinity of IPs to sustain favorable experimental conditions during the whole store.

2. Minimization of radiation impact on personnel and the environment by localizing beam loss in the pre-determined regions and using appropriate shielding in these regions.
3. Protection of accelerator components against irradiation caused by operational beam loss and enhancement of reliability of the machine.
4. Prevention of quenching of SC magnets and protection of other machine components from unpredictable abort and injection kicker prefires/misfires and unsynchronized aborts.

BEAM LOSS AND SCRAPING RATES

Although beam loss and scraping rates depend on the machine specifics, their origin and values have much in common at hadron colliders. They are reliably estimated for the Tevatron [3, 4]. The ultimate Run II parameters include 36 bunches of 2.7×10^{11} protons and 1.35×10^{11} antiprotons each, with normalized horizontal emittances of 20 mm-mrad and 15 mm-mrad, respectively. The total beam intensities at the beginning of the store are $N_p = 9.72 \times 10^{12}$ and $N_{\bar{p}} = 4.86 \times 10^{12}$. The ultimate luminosity at the beginning of the store would be $3.31 \times 10^{32} \text{ cm}^{-2}\text{s}^{-1}$ averaging to $1.43 \times 10^{32} \text{ cm}^{-2}\text{s}^{-1}$ over a 13.5-hour store. Estimated evolution of beam loss ΔI over such a store for three major components is as following:

1. $\bar{p}p$ collisions at two IPs (*collision loss*), $\Delta I = 2.2 \times 10^7 \text{ p/s}$ or \bar{p}/s .
2. Particle loss from the RF bucket due to heating of a longitudinal degree of freedom (*longitudinal loss*),

¹ This work was supported by the Universities Research Association, Inc., under contract DE-AC02-76CH03000 with the U.S. Department of Energy.

² mokhov@fnal.gov

$\Delta I = 2 \times 10^7$ p/s and 6.1×10^6 \bar{p} /s.

3. *Beam-gas scattering*, $\Delta I = 6.5 \times 10^6$ p/s and 2.9×10^6 \bar{p} /s, calculated at a nitrogen equivalent pressure of 10^{-9} torr with the following gas content (in nanotorr): H₂ (5.7), CO (0.14), N₂ (0.07), C₂H₂ (0.06), CH₄ (0.11), CO₂ (0.07), Ar (0.09).

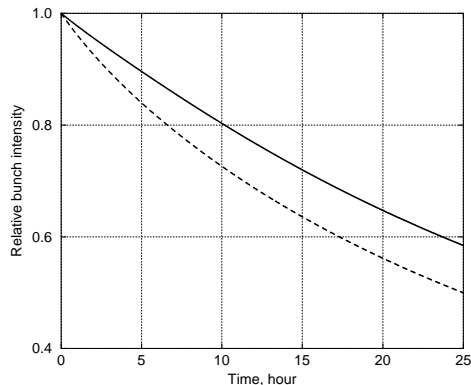


FIGURE 1. Relative bunch intensity as evolved in a Tevatron store for protons (solid) and antiprotons (dashed).

Fig. 1 shows beam intensity decay over a store. Inelastic and 60% of elastic events contribute to *collision loss*, because about 40% of protons (antiprotons) elastically scattered at the Tevatron IPs remain in the 3σ core after a bunch-bunch collision. Intensity drops over a 13.5-hour store are 26% and 34% for proton and antiproton beams, respectively. Longitudinal beam loss, beam gas-scattering and elastic part of collision loss are the main mechanisms of the *slow beam halo growth*. The main collimation system is designed to intercept about 99.9% of this halo, with $N_{sp} = 2.93 \times 10^7$ p/s and $N_{s\bar{p}} = 1.15 \times 10^7$ \bar{p} /s as the scraping rates for proton and antiproton beams, correspondingly.

TWO-STAGE COLLIMATION

The most direct way of collimating a beam of particles is to define the physical aperture with a solid block of absorbing material. In the early Tevatron days the first collimation system was designed [5] on the basis of simulations with the MARS and STRUCT codes [6, 7]. The optimized system, which consisted of a set of collimators about 1 m long each, was installed in the Tevatron, that immediately made it possible to raise by a factor of five the efficiency of the fast resonant extraction system and intensity of the extracted 800 GeV proton beam. The data on beam loss rates and their dependence on the collimator jaw positions were in excellent agreement with the calculation predictions.

Depending upon the energy, material and thickness, a certain fraction of the intercepted beam will survive, either be traversing the whole length of the block or by being scattered out of the block. The first component can be reduced by using a longer jaw or a denser material. Suppression of the outscattered particles is much more difficult. For a given material, their yield depends upon the impact parameter Δ and particle energy. Δ grows linearly with the halo transverse diffusion velocity v . At Tevatron, v is about $1.5 \mu\text{m/s}$ and $\Delta = 0.1\text{-}0.5 \mu\text{m}$. This results in a probability of outscattering close to 0.5, *i.e.*, low collimation efficiency.

A natural way to catch the outscattering particles is by switching to a *two-stage collimation* system. The whole system consists then of a primary *thin scattering target*, followed by a few *secondary collimators* at the appropriate locations in the lattice. The purpose of a thin target is to increase the amplitude of the betatron oscillations of the halo particles and thus to increase their impact parameter Δ on the secondary collimators on the next turns, without influencing the unscattered beam. At Tevatron, $\Delta \approx 0.1\text{-}0.3$ mm on secondary collimators – almost a factor of 1000 larger than on the primary ones. This results in a significant decrease of the outscattered proton yield, total beam loss in the accelerator and jaw overheating, mitigating requirements to collimator alignment. Besides that, the collimation efficiency becomes almost independent of accelerator tuning. There is only one significant but totally controllable restriction of the accelerator aperture and only the secondary collimator region needs heavy shielding.

In 1995, based on the MARS-STRUCT simulations, the existing scraper in the Tevatron at A \emptyset was replaced with a new one with two 2.5-mm thick L-shape tungsten targets with a 0.3-mm offset relative to the inner surface on either end of the scraper (to eliminate the misalignment problem). This resulted in reduction of beam loss rate upstream of both collider detectors by a factor of five, in agreement with the modeling predictions [8]. The system was further improved for Run II [9] (see below).

Two-stage collimation systems were parts of the original designs in all the superconducting hadron collider projects: 3 \times 3-TeV UNK at Protvino [10], 20 \times 20-TeV SSC in Texas [1, 2], 7 \times 7-TeV LHC at CERN [11, 12], 0.82-TeV proton HERA ring at DESY [13], 20 \times 20-TeV (Stage-1) and 88 \times 88-TeV (Stage-2) VLHC in Illinois [14].

POSITIONING AND DESIGNING COLLIMATORS

Thin movable primary collimators (*scatterers, targets, blades*) are optimized for the beam and heating (scatter-

ing, integrity and cooling) and positioned at $x_0 = m\sigma_0$ from the beam axis ($m \approx 5$) in a high- β (*betatron cleaning*) and non-zero dispersion (*momentum cleaning*) regions, three in total: horizontal, vertical and off-momentum. Movable secondary collimators (e.g., L-shape jaws) – long enough to absorb showers induced by particles scattered from the primary collimators – are located at the appropriate phase advances $\Delta\phi$ at $x = n\sigma$ from the beam axis. Here, σ_0 and σ are the beam RMS at the entrance to the primary and secondary collimators, respectively, for each plane. The secondary collimator jaws are aligned parallel to the envelope of the circulating beam.

The optimum conditions for the positioning the secondary collimators with respect to the scatterer is determined from [1]

$$\Delta\phi = \pi k \pm \arccos(m/n),$$

$$n - m > |\Delta p/p(\eta_0/\sigma_0 - \eta/\sigma)| + \delta,$$

where $k = 0, 1, 2, \dots$, η_0 and η are dispersions at the primary and secondary collimator positions, respectively, and $\delta \sim 1$. The favorable condition is to have the secondary collimator jaw on the same side of the beam as the primary collimator, which results in the optimal phase advances $\Delta\phi = 20\text{-}40^\circ$ and $300\text{-}320^\circ$ for the horizontal scraping, and $\Delta\phi \sim 40^\circ$ and $140\text{-}160^\circ$ for the vertical scraping. For the primary and secondary jaws positioned at the opposite sides of the beam ($n > 0, m < 0$) and for $n - m < 1$, the optimal phase advance is about 160° . Fortunately, there is no strong dependence of the collimation efficiency on the phase advance in the above ranges of $\Delta\phi$, which leaves freedom to vary collimator positions to match the other requirements [1].

The following design constraints are taken into account while developing and engineering a collimation system at a hadron collider:

- Minimum outscattering from a primary-secondary collimator couple.
- Impedance constraints.
- The apertures do not occlude any beam when in the garage position.
- No quench of downstream superconducting magnets.
- Muon vectors downstream do not create any problem to the experiments and environment.
- Local shielding (if needed) provides protection of ground water and equipment around the unit, and residual dose rate on its outside below 1 mSv/hr.
- Target/jaw material integrity and cooling issues.
- Alignment issues.

TEVATRON RUN II

The Tevatron Run II collimation system [9] is based on a two-stage approach to localize most of beam losses in the straight sections D49, E0 and F17. Collimator positions in the ring are shown in Fig. 2. Parameters of the scatterers and secondary collimators have been carefully optimized for the 1-TeV proton and antiproton beams. The 5-mm thick tungsten primary collimators are positioned at 5σ from the beam axis both in vertical and horizontal planes. The 1.5-m long stainless steel secondary collimators consist of L-shape jaws positioned at 6σ from the beam axis in both planes. Numerical simulations were done for the lattice in the presence of the proton and antiproton orbit separation designed for Run II.

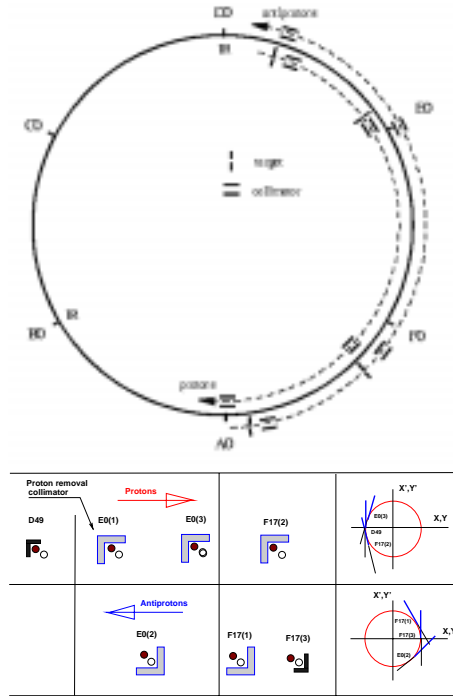


FIGURE 2. Tevatron Run II beam collimation system.

Large amplitude protons are intercepted by the secondary collimators during the first turn after interaction with the primary collimator. Protons (antiprotons) with amplitudes smaller than 6σ survive during several tens of turns until they increase amplitude in the next interactions with primary collimators. These particles produce a secondary halo and occupy the 6σ envelope. Beam halo particles interact with primary collimators 2.2 times on average. About 0.1% of protons and antiprotons hitting the secondary collimator jaws are scattered back into the beam pipe and later lost on limiting apertures, in most cases upstream of the CDF and D0 collider detectors. Products of beam-gas interactions not intercepted by the

collimation system also have a good chance to be lost at the same locations in front of the IPs. The main process of beam-gas interaction, a multiple Coulomb scattering, results in slow diffusion of protons (antiprotons) from the beam core causing emittance growth. These particles increase their betatron amplitudes gradually during many turns and are intercepted by collimators before they reach other limiting apertures. In inelastic nuclear interactions of a beam with residual gas, leading nucleons are generated at angles large enough for them – along with other secondaries – to be lost within tens of meters after such interactions.

Overall, this system provides effective beam cleaning of slowly growing transverse and longitudinal halo, reliably protecting the machine and detectors. It was shown in Ref. [4] that with the Tevatron parameters, nuclear elastic beam-gas scattering can result in a substantial increase of the betatron amplitude. Beam loss distribution due to this process follows the vacuum distribution (Fig. 3). It turns out that a fraction of these particles is not intercepted by the main collimators, and about 25% of them are lost in the vicinity of the IPs adding to the detector background. Moreover, unacceptable beam loss happens in the BØ low- β region at the abort kicker pre-fire, resulting in the SC magnet quench and severe damage to the CDF silicon detectors. To cure this, a 0.5-m long steel mask is installed this summer immediately upstream of the last three dipoles before BØ, with its parameters carefully optimized in detailed MARS-STRUCT simulations [15, 16].

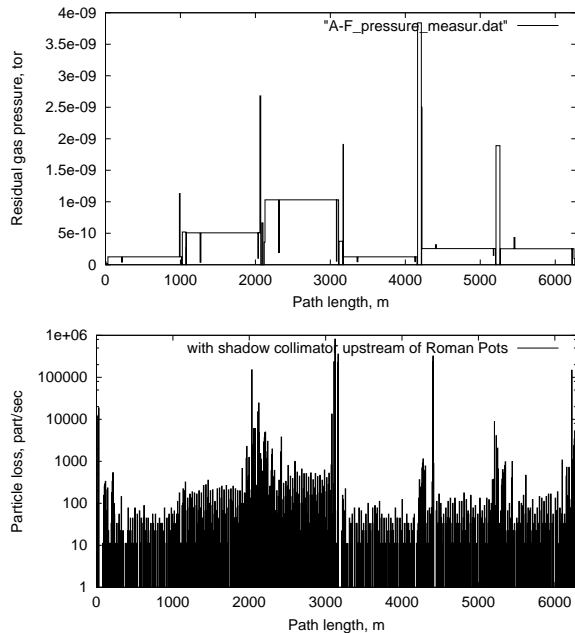


FIGURE 3. Measured residual gas pressure (*top*) and STRUCT-calculated beam loss distribution from nuclear elastic beam-gas scattering (*bottom*).

CRYSTAL COLLIMATION

It was shown for the first time in Ref. [1] that replacing an amorphous primary collimator with a bent crystal can drastically improve the collimation efficiency for TeV beams. A channeling crystal coherently deflects a fraction of the beam halo, directing it, as a whole, deeper into a second collimator body, substantially reducing the outscattering probability. Detailed CATCH-STRUCT calculations [17] have shown that at the Tevatron, beam loss rates in the critical IP locations can be reduced by a factor of ten (see Table 1). Moreover, a number of inelastic nuclear interactions in the optimal crystal is about four times lower compared to that in the optimal amorphous target, that reduces radiation load to the downstream SC magnets by the same factor.

TABLE 1. Halo hit rates at the Fermilab DØ and CDF Roman pots and nuclear interaction rates N in target and crystal (in $10^4 p/s$)

	With target	With crystal		
		Amorphous layer thickness		
		10 μm	5 μm	2 μm
DØ	11.5	1.35	1.60	1.15
CDF	43.6	5.40	3.20	3.43
N	270	82.4	70.6	50.3

HERA

It was shown in a detailed study [13] that a single collimator was insufficient in removing the beam halo responsible for the background rates in the H1 and ZEUS detectors at HERA. It has been demonstrated – both by Monte Carlo simulations and experimentally – that these backgrounds can be significantly reduced by installing a two-stage collimation system. Depending on beam lifetime, reduction factors of up to 10 have been observed in dedicated experiments.

Like at Tevatron, the beam-gas induced part of the hadronic background constitutes a constant radiation level that is not affected by the collimators. Recently, another source of the background was discovered at HERA, the C5 mask [18]. The mask's main purpose is to shield from backscattered synchrotron radiation from the lepton beam. However, it is also a scattering source for protons. Reconstruction of the IP location revealed many events coming from this mask located about 0.8 m downstream (as seen by the lepton beam) of the IP. So, it will be made thinner. Another issue was not well pumped Zinc found in the H1's copper-coated tungsten mask. The masks have been replaced and tested to be Zinc-free. Other activities by the machine-detector interface group take place HERA to reduce backgrounds [18].

LHC

At nominal operation parameters, each of the 7 TeV circulating beams of the LHC contains approximately 334 MJ of energy, which is enough to cause severe damage to the expensive machine and detector equipment. An extremely reliable abort system will use fast extraction to divert the beam to an external graphite absorber at the end of a normal fill or in case of a detected anomaly in beam behavior. There are three collimation systems implemented into the complex: high-luminosity interaction region protection, beam cleaning system and protection at beam accidents.

The high-luminosity IR protection system on each side of the IP1 and IP5 has been designed over the years on the basis of comprehensive MARS calculations [19]. It includes:

- The TAS front copper absorber at $L=19.45$ m from the IP (1.8 m long, 34-mm ID, 500-mm OD).
- A 7-mm thick stainless steel (SS) liner in the Q1 quadrupole.
- The SS absorber TASB at $L=45.05$ m (1.2-m long, $r=33.3-60$ mm).
- A ~ 3 -mm thick SS liner in the Q2A through Q3 quadrupoles.
- 40-cm long SS masks at $L=23.45$ m, $r=250-325$ mm to protect the Q1 slide bearings.
- The neutral particle 3.5-m copper absorber TAN at 140 m from the IP.
- The 1-m long TCL SS collimator at 191 m from IP.

This system, developed under realistic engineering constraints, will protect the LHC IP1/IP5 region components against luminosity-driven short- and long-term deleterious energy deposition effects with a good safety margin, at least at the design luminosity of $10^{34} \text{ cm}^{-2}\text{s}^{-1}$, not compromising the physics both in the main (CMS and ATLAS) and forward (TOTEM) detectors.

The beam cleaning system occupies two dedicated insertions for momentum cleaning in IR3 (1 primary and 6 secondary), and betatron cleaning in IR7 (4 primary and 16 secondary), with 54 movable collimators total for two rings. The system layout has been worked out to provide the required cleaning efficiency of 99.998% and integrated into the machine. Open questions still remain [20]: foreseen collimator materials do not withstand the expected beam impact (require a factor of 100-200 better resistance); impedance from collimators is critical; mechanical and operational tolerances are tight; high activation imposes severe restrictions on hands-on maintenance.

Protection at beam accidents. A beam loss, caused by an unsynchronized abort launched at abort system malfunction, can cause severe damage to collider inner triplet components and the CMS detector near-beam elements. A set of stationary collimators for the IP5 interaction region has been proposed in [21] to protect its elements and mitigate consequences to the detector. Fig. 4 gives details of the MARS model of the system. The first collimator is positioned at $21\sigma_{collis}=10.3\sigma_{inject}=10$ mm from the beam orbit (11.8 mm from the beam pipe center). Second and third collimators are used to protect magnets from secondary particles emitted from the first one. The collimator configuration, materials and dimensions have been carefully optimized to provide reliable protection of the inner triplet and to ensure collimator survivability. Combined with an unsynchronized abort, such a system reduces peak energy deposition in the IP5 inner triplet quadrupoles by almost six orders of magnitude compared to the disastrous case of a 1-module pre-fire.

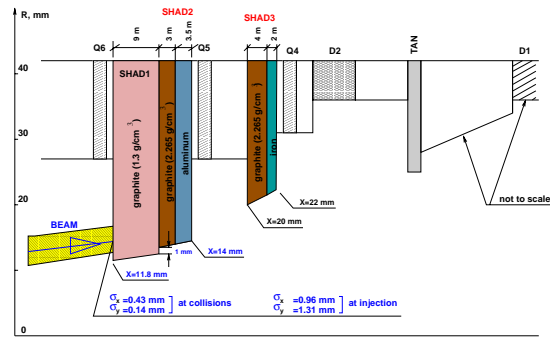


FIGURE 4. Stationary collimators in the LHC IP5 outer triplet.

Alternatively, a movable collimator system in the IP6 beam abort straight section, as close to the cause as possible, has been proposed in [22] to protect the entire LHC machine. The configuration of the system is similar to the one shown in Fig. 4. A composite 9.5-m long graphite (8 m) and aluminum (1.5 m) collimator TCDQ is placed at a radial position of 9.1 mm, corresponding to $8\sigma_x$ of the circulating beam at collision energy of 7 TeV, plus orbit deviations. It is movable, *i.e.* the jaws are retracted at injection to accommodate a larger beam size. The studies revealed that with this system, the entire machine and detector components are reliably protected against any damage at an unsynchronized beam abort. The peak temperature rise in the IP6 components is quite acceptable. If the abort kicker delay time exceeds $1 \mu\text{s}$, several first SC quadrupoles and dipoles in the IP6 can quench. Two additional movable 2-m steel masks are added between the Q5 quadrupole and SC dipoles to reduce the length of the quench region to less than 50% of the first string.

VLHC

The collimation system [14], designed for the 20×20 -TeV Stage-1 VLHC, consists of horizontal and vertical primary collimators and a set of secondary collimators placed at optimal phase advances. From the very beginning, the lattice was designed to provide a warm collimation region with enough space to accommodate the system and provide large dispersion for those collimators which intercept the off-momentum protons. The primary collimators are positioned at 7σ while secondary ones are at 9.2σ from the beam axis. Eight supplementary collimators are placed in the next long straight section to decrease particle losses in the low- β quadrupoles. These collimators are positioned at $14\sigma_{x,y}$ to intercept particles outscattered from the secondary collimators. There are only several SC magnets in the arcs with beam loss rate of 0.3 to 1 W/m, the rest of the arc is clean. Total beam loss in the low- β quadrupoles, induced by the tails from collimators, is 61 W. Adding the supplementary collimators, one reduces this by about an order of magnitude.

CONCLUSIONS

Two-stage collimation, proven to work at Tevatron and HERA, requires further R&D to improve its efficiency, and meet LHC and VLHC challenges – under realistic halo and beam loss scenarios and engineering constraints, and exploring novel techniques.

REFERENCES

1. Maslov, M. A., Mokhov, N. V., and Yazynin, I. A., The SSC Beam Scraper System, Tech. rep., SSCL-484 (1991).
2. Drozhdin, A. I., Mokhov, N. V., Soundranayagam, R., and Tompkins, J., Toward Design of the Collider Beam Collimation System, Tech. rep., SSCL-Preprint-555 (1994).
3. Mokhov, N. V., and Balbekov, V. I., *Handbook of Accelerator Physics and Engineering, 2nd Printing*, Ed. A. W. Chao and M. Tigner, World Scientific, 218–220 (2002).
4. Drozhdin, A. I., Lebedev, V. A., Mokhov, N. V., Nicolas, L. Y., Sidorov, D. V., Striganov, S. I., and Tollestrup, A. V., Beam Loss and Backgrounds in the CDF and DØ Detectors due to Nuclear Elastic Beam-Gas Scattering, Tech. rep., Fermilab-FN-734 (2003).
5. Drozhdin, A. I., Harrison, M., and Mokhov, N. V., Study of Beam Losses During Fast Extraction of 800-GeV Protons from the Tevatron, Tech. rep., Fermilab-FN-418 (1985).
6. Mokhov, N. V., Status of MARS Code, Tech. rep., Fermilab-Conf-03/053 (2003).
7. Baishev, I. S., Drozhdin, A. I., and Mokhov, N. V., STRUCT Program User's Reference Manual, Tech. rep., SSCL-MAN-0034 (1994).
8. Butler, J. M., Denisov, D. S., Diehl, H. T., Drozhdin, A. I., Mokhov, N. V., and Wood, D. R., Reduction of Tevatron and Main Ring Induced Backgrounds in the DØ Detector, Tech. rep., Fermilab-FN-629 (1995).
9. Church, M. D., Drozhdin, A. I., Legan, A., Mokhov, N. V., and Reilly, R. E., "Tevatron Run-II Beam Collimation System," in *1999 Particle Accelerator Conf.*, IEEE Conference Proceedings Fermilab-Conf-99/059, New York, 1999, pp. 56–58.
10. Drozhdin, A. I., Maslov, M. A., and Mokhov, N. V., "Protection of the UNK Superconducting Ring Against Irradiation at Beam Collimation," in *X All-Union Conference on Charged Particle Accelerators*, Proceedings, vol. 2, JINR, Dubna, 1987, pp. 278–285.
11. Burnod, L., and Jeanneret, J. B., Beam Losses and Collimation in the LHC: A Quantative Approach, Tech. rep., CERN SL/91-39 (1991).
12. Trenkler, T., and Jeanneret, J. B., The Principles of the Two-stage Betatron and Momentum Collimation in Circular Accelerators, Tech. rep., CERN SL/95-03 (AP), LHC Note 312 (1995).
13. Seidel, M., The Proton Collimation System of HERA, Tech. rep., DESY 94-103 (1994).
14. Mokhov, N. V., Drozhdin, A. I., and Foster, G. W., "Beam-Induced Energy Deposition Issues in the Very Large Hadron Collider," in *2001 Particle Accelerator Conf.*, IEEE Conference Proceedings Fermilab-Conf-01/135, Chicago, 2001, pp. 3171–3173.
15. Church, M. D., Drozhdin, A. I., Moore, R. S., and Still, D. A., Tevatron Abort Kicker Prefire Simulations, Tech. rep., Fermilab Beams-doc-648 (2003).
16. Nicolas, L. Y., and Mokhov, N. V., Impact of the A48 Collimator on the Tevatron B0 Dipoles, Tech. rep., Fermilab-TM-2214 (2003).
17. Biryukov, V. M., Drozhdin, A. I., and Mokhov, N. V., "On Possible Use of Bent Crystal to Improve Tevatron Beam Scraping," in *1999 Particle Accelerator Conf.*, IEEE Conference Proceedings Fermilab-Conf-99/072, New York, 1999, pp. 1234–1236.
18. Minty, M., *Private Communication*, DESY (2003).
19. Mokhov, N. V., Rakhno, I. L., Kerby, J. S., and Strait, J. B., Protecting LHC IP1/IP5 Components Against Radiation Resulting from Colliding Beam Interactions, Tech. rep., Fermilab-FN-732, LHC Project Report 633 (2003).
20. Assmann, R., "Designing and Building a Collimation System for the High-Intensity LHC Beam," in *2003 Particle Accelerator Conf. Proceedings*, Portland, Oregon, 2003.
21. Drozhdin, A. I., Mokhov, N. V., and Huhtinen, M., "Impact of the LHC Beam Abort Kicker Prefire on High Luminosity Insertion and CMS Detector Performance," in *1999 Particle Accelerator Conf.*, IEEE Conference Proceedings Fermilab-Conf-99/060, New York, 1999, pp. 1231–1233.
22. Mokhov, N. V., Drozhdin, A. I., Rakhno, I. L., Gyr, M., and Weisse, E., "Protecting LHC Components Against Radiation Resulting from an Unsynchronized Beam Abort," in *2001 Particle Accelerator Conference*, IEEE Conference Proceedings Fermilab-Conf-01/133, Chicago, 2001, pp. 3168–3170.